

PNAS

www.pnas.org

Supplementary Information for

Artificial athletic turf infill associated with systematic toxicity in an amniote vertebrate

Elvis Genbo Xu, Nicholas Lin, Rachel S. Cheong, Charlotte Ridsdale, Rui Tahara, Trina Y. Du, Dharani Das, Jiping Zhu, Laura Peña Silva, Agil Azimzada, Hans C. E. Larsson, Nathalie Tufenkji

Correspondence to: Hans C. E. Larsson, Nathalie Tufenkji
Email: hans.ce.larsson@mcgill.ca; nathalie.tufenkji@mcgill.ca

This PDF file includes:

- Supplementary text
- Figs. S1 to S6
- Tables S1 to S5
- References for SI reference citations

Supplementary Information Text

Methods

Nano-CT scan analysis by Dragonfly. The scanned samples were analyzed with Dragonfly image analysis software (Object Research Systems Inc.). A number of linear measurements were taken for brain morphometric analysis and 3-Dimensional volumes of the brain tissue were manually segmented with Dragonfly. Three-Dimensional meshes of the exterior and interior surfaces from six randomly selected brains of injected embryos (three controls and three treated) were generated from the segmented CT scans. MeshLab (1) was used to remove isolated faces, close holes in the meshes, and limit the volumes to the posterior margin of the mesencephalon because of slight twisting in the brain stem. Meshes were subsampled in MeshLab using the Poisson-disk sampling algorithm (2) set to 5000 samples, then re-meshed using the Screen Poisson surface reconstruction algorithm (3). To reduce artifacts in subsequent comparisons, brains with a significant degree of asymmetry were sagittally bisected and mirrored before subsampling and remeshing. Point-to-point correspondence and alignment of meshes were established using the “geomorph” package for R (4). The “digitsurface” function was used to digitize five fixed landmarks and 400 surface semilandmarks, and the “gpagen” function was used to align the surfaces using a full Procrustes superimposition. The thin-plate spline method (5) implemented by the “warpRefMesh” function in “geomorph” was used to warp a template surface mesh file into the shapes of the mean control and treatment brains calculated from the digitized landmarks. The vector map of surface differences between groups was generated using the “ModelToModelDistance”

module in 3-D Slicer (6). Brain thickness was calculated by following the same procedure and comparing the distance between interior and exterior surfaces.

Determination of metals. Inductively coupled plasma mass spectrometry (ICP-MS) (NexION 300X, Perkin Elmer) was used to determine the metal content (Al, Cr, Cu, Zn, As, Cd, and Pb) in the CR leachate and embryonic tissue samples. For CR leachate digestions (triplicate), 1 mL aliquots of the leachate were mixed with 1 mL of 67-70 % HNO₃ (ultratrace grade, BDH Aristar Ultra) in polypropylene tubes and were digested for 16 hours at 85 °C using DigiPREP digestion system (SCP Science). For tissue samples, digestions were conducted under identical conditions, following the addition of 1 mL of 67-70 % HNO₃ and 0.5 mL of Milli-Q water (resistivity > 18.2 MΩ.cm, organic carbon <2 µg C L⁻¹) to pre-weighed tissues (~150-250 mg) of brain, heart, liver, yolk, and albumin. Following the digestions, the sample volumes were completed to 10 mL with Milli-Q water and well vortexed for 1 min at 3000 rpm, before the subsequent 5 times dilution (with a final 2 % v/v HNO₃). The calibrations (dual detector) were built using IV-ICP-MS-71A multi-element standards (Inorganic Ventures) based on the isotope analysis of Al-27, Cr-52, Cu-63, Zn-66, As-75, Cd-111 and Pb-208. To account for the signal alterations due to possible matrix effects, the internal standards (IS) of Sc-45 (for Al, Cr, Cu and Zn), Y-89 (for As), In-115 (for Cd) and Bi-209 (for Pb) were used to correct the analyte signals (with the IS recovery obtained between 90 % and 110 %). The calibrations were re-built after every 20 samples, in order to minimize any instrumental signal drift over time in the cases of big-batch analyses. The quality of the measurements was tested against the blank (Milli-Q water with 2 % v/v HNO₃), QCS-27 standard

(High-Purity Standards), Trace Metals in Drinking Water Standard (TMDW, High-Purity Standards) as well as the calibration standards after every 10 samples, with the observed deviations not exceeding $\pm 5\%$.

Gas chromatography and mass spectrometry (GC/MS) analysis. GC/MS analysis was carried out using an Agilent gas chromatograph (Model: 7890A; Santa Clara, CA) connected to a Triple-Quad mass spectrometer (Agilent Technology Ltd., Model: 7000A; Santa Clara, CA) and a Gerstel Multi-Purpose MPS autosampler (MPS 2XL; GERSTEL GmbH & Co., Germany). For the qualitative analysis, a 30 m long DB-1MS capillary column (Agilent Technology Ltd.; Santa Clara, CA) with 0.25 mm internal diameter and 0.25 μm film thickness was used. The column flow was kept constant at 1.2 mL/min of helium and the injector was operated in splitless mode. The initial GC oven temperature was set at 35 °C and initial hold time of 2 min. Then the temperature was raised at a rate of 10 °C/min to 300 °C and held for 15 min. The injector temperature was kept at 270 °C and the transfer line between the GC and MS were heated to 300 °C. The MS conditions were as follows: Source temperature: 230 °C; Quad 1 and 2: 150 °C and the ions (m/z) were scanned in the range of 33 to 500. Samples were analyzed in both electron impact (EI) and in chemical ionization (CI; methane as the collision gas) modes. The spectra obtained in EI mode were used for compound identification purposes by comparing their mass spectral profiles with those present in the National Institute of Standards and Technology (NIST) database. The spectra obtained in CI mode were used for further confirmation of results obtained in the EI mode. For quantitative analysis, a 30 m long CAM column (Agilent Technology Ltd., Santa Clara, CA) with 0.25 mm internal diameter and 0.25 μm film thickness was used. The column flow was kept constant at 1.2

ml/min of helium and the injector was operated in splitless mode. The initial GC oven temperature was set at 35 °C and initial hold time of 2 min. Then the temperature was raised at a rate of 10 °C/min to 200 °C and held for 10 min. The injector temperature was kept at 270 °C and the transfer line between the GC and MS were heated at 300 °C. The MS conditions were as follows: Source temperature: 230 °C; Quad 1 and 2: 150 °C. A multiple reaction monitoring (MRM) method was utilized to analyze and quantitate the amines in the extracts. The chemical names, corresponding ion transitions for quantitation and the MRM conditions are shown in **Table S5**. To minimize the effect of the matrix on the quantification, all calibration standards were prepared by adding the proper amount of amines into 10 mL of LC/MS grade water. The standards were extracted in the same way as the leachate samples. All peak areas of amines in the calibration standards and in the samples were normalized to the internal standard for the final calculation of concentrations.

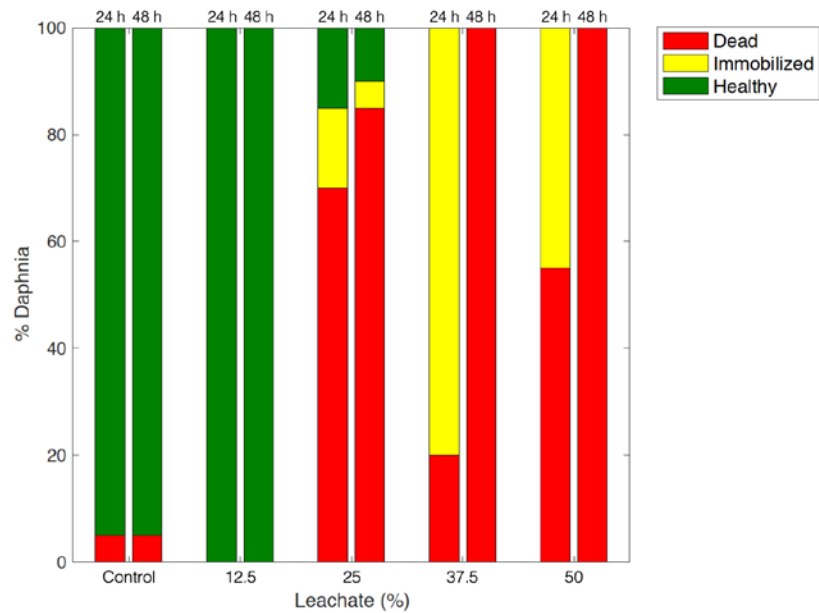


Fig. S1.

Concentration-dependent mortality and immobility of *Daphnia magna* after crumb rubber leachate exposure. *Daphnia* neonates less than 24 h old were exposed to control, 12.5 %, 25 %, 37.5 %, and 50 % crumb rubber water leachate for 24 h and 48 h. The animal culture and exposure methods follow OECD (7).

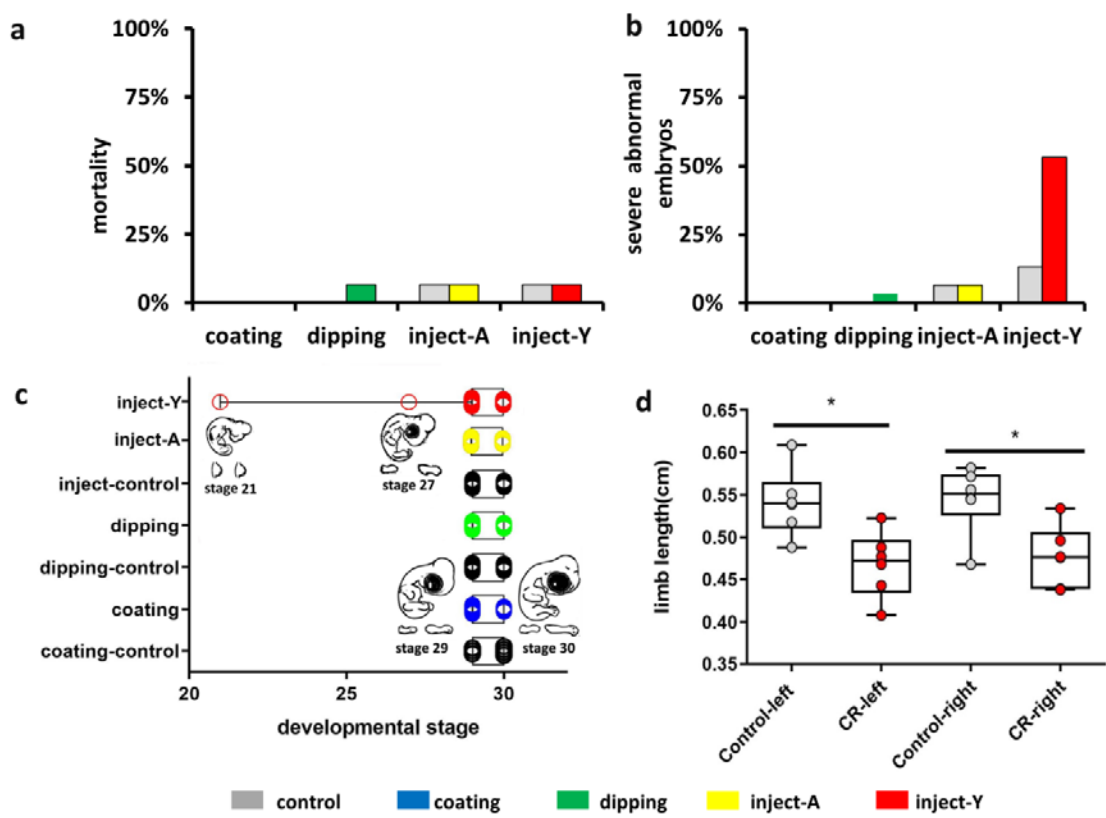


Fig. S2.

The effects of 100% crumb rubber water leachate on (a) the mortality, (b) percentage of severe abnormality, (c) developmental stage, and (d) mean limb length on E7 chicken embryos. * $p < 0.05$ (one-way ANOVA followed by Bonferroni's t-test; $n = 30$ for coating and dipping, $n = 15$ for inject-A and inject-Y). Inject-A, E0 embryos were injected with CR leachate into the air cell; inject-Y, E0 embryos were injected with CR leachate into yolk. Control E0 embryos were treated with LC/MS grade water with the same application methods.

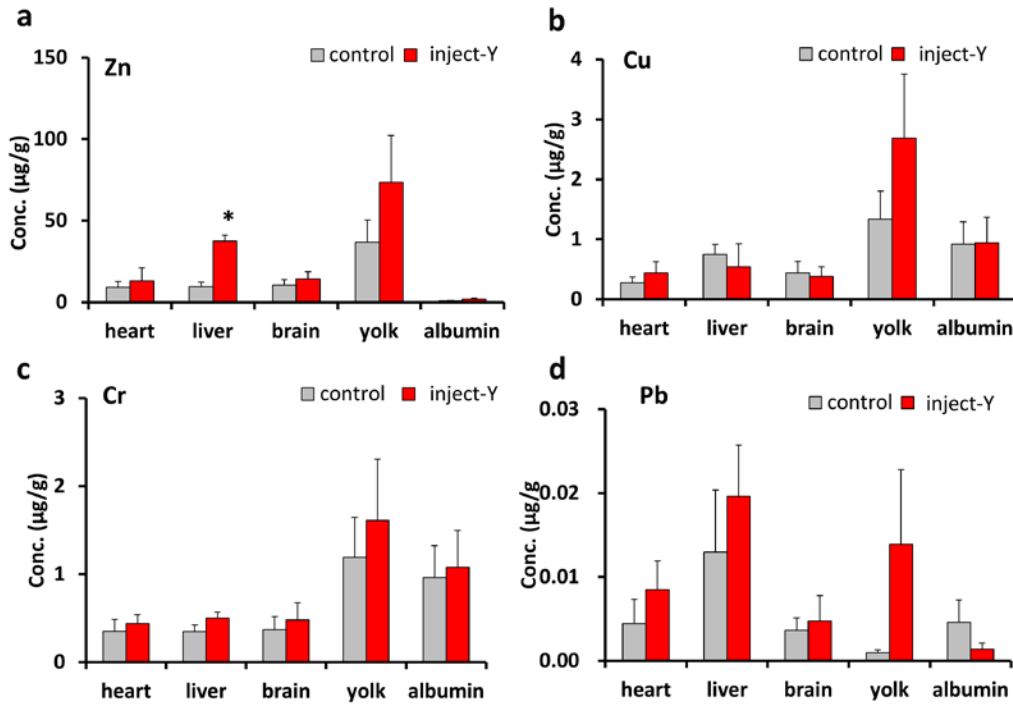


Fig. S3.

The concentration of detected metals (Zn, Cu, Cr, and Pb) in the heart, liver, brain, yolk, and albumin of control and inject-Y E7 chicken embryos. * $p < 0.05$ (t-test; $n = 3$; each sample is pooled from 3-5 chicken embryos). Control, E0 embryos were injected with LC/MS grade water into yolk; inject-Y, E0 embryos were injected with CR leachate into yolk.

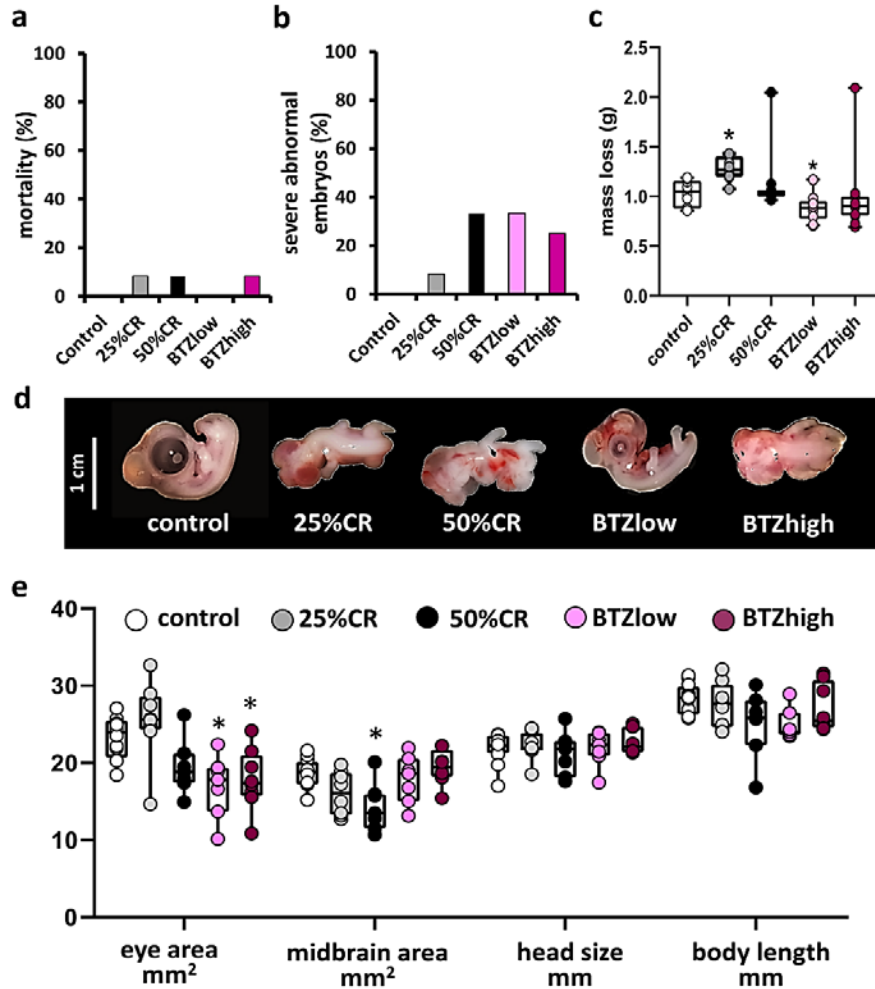


Fig. S4.

The effects of crumb rubber water leachate and benzothiazole (BTZ) on the growth and general morphology of E7 chicken embryos. (a) Mortality. (b) Percentage of severe abnormal embryos. (c) Egg mass loss. (d) Embryos exhibit severe malformations. (e) Measurements of the eye area, midbrain area, head size, and body length. 25%CR, E0 embryos were injected with 25% CR leachate into the yolk; 50%CR, E0 embryos were injected with 50% CR leachate into the yolk; BTZlow, E0 embryos were injected with 1.5 mg/L BTZ into the yolk; BTZhigh, E0 embryos were injected with 15 mg/L BTZ into the yolk; control E0 embryos were treated with LC/MS grade water with the treatment-equivalent methods. * $p < 0.05$ (one-way ANOVA followed by Tukey test; $n = 12$).

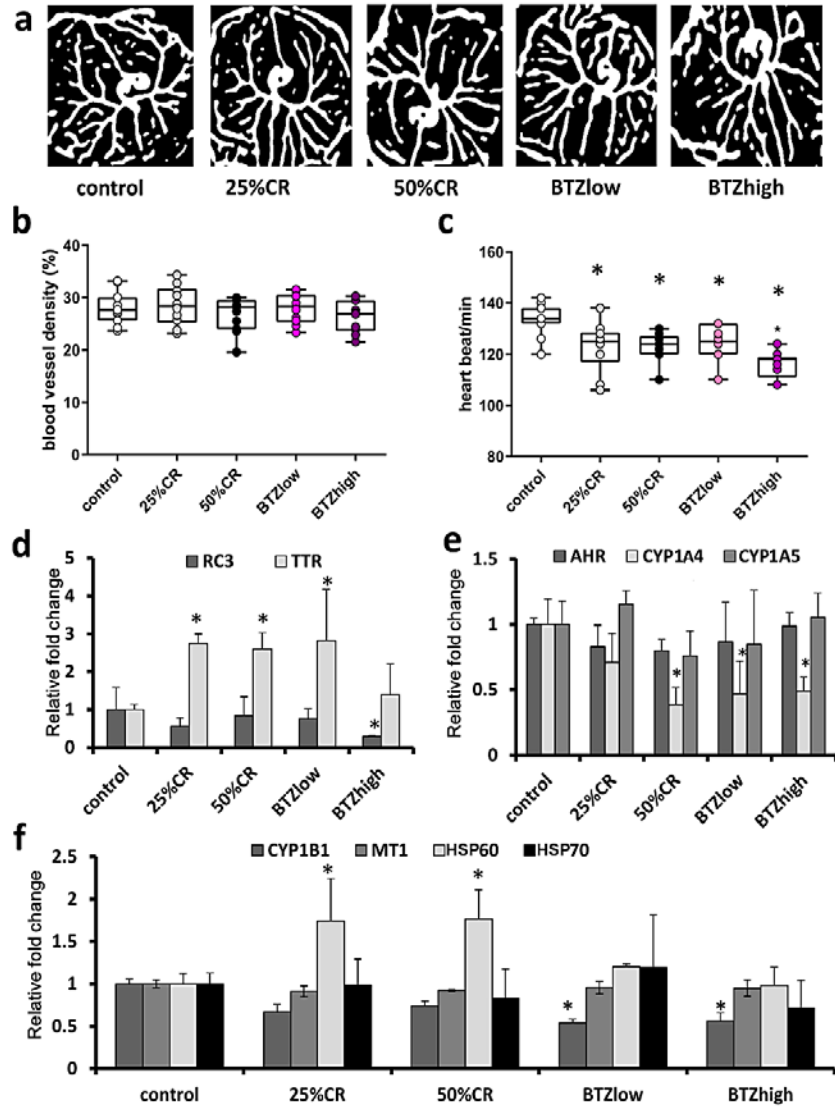


Fig. S5.

The effects of crumb rubber water leachate and benzothiazole (BTZ) on embryonic angiogenesis, heartbeat, and gene expression of chicken embryos. (a) Representative images of developing blood vessels of control and treated E3 embryos. (b) Blood vessel density of E3 embryos. (c) Heartbeat rate of E3 embryos. * $p < 0.05$ (one-way ANOVA followed by Tukey test; $n = 12$). Gene expression in brain (d), liver (e), and heart (f) of E7 embryos. * $p < 0.05$ (one-way ANOVA followed by followed by Tukey test; $n = 6$). Control, E0 embryos were injected with LC/MS grade water into yolk; 25%CR, E0 embryos were injected with 25% CR leachate into the yolk; 50%CR, E0 embryos were injected with 50% CR leachate into the yolk; BTZlow, E0 embryos were injected with 1.5 mg/L BTZ into the yolk; BTZhigh, E0 embryos were injected with 15 mg/L BTZ into the yolk.

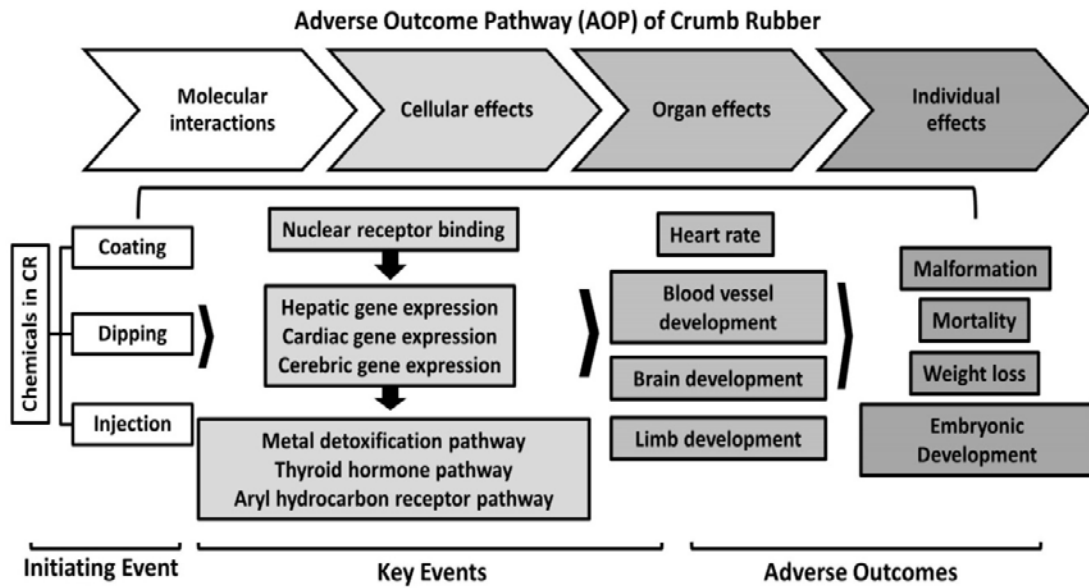


Fig. S6. An adverse outcome pathway (AOP) framework of crumb rubber in the chicken embryo model.

Table S1.

Concentration of metals detected in the crumb rubber water leachate.

	Average ($\mu\text{g/L}$)	SD (n = 3)
Al	5.71	0.07
Cr	1.81	0.11
Cu	7.47	0.16
Zn	5156.26	25.81
As	2.32	0.03
Cd	0.02	0.008
Pb	0.29	0.004

Table S2.

Organic compounds detected in the crumb rubber water leachate.

Chemical Name	Formula	% of total	Concentration ($\mu\text{g/L}$)*
4-Methyl-2-pentanamine	$\text{C}_6\text{H}_{15}\text{N}$	3.5	352
Cyclohexylamine	$\text{C}_6\text{H}_{13}\text{N}$	8.3	838
N-Butyl-1-butamine	$\text{C}_8\text{H}_{19}\text{N}$	0.3	34
N,N-Dimethylcyclohexanamine	$\text{C}_8\text{H}_{17}\text{N}$	0.5	49
N-ethyl-4-methyl-2-pentanamine	$\text{C}_8\text{H}_{19}\text{N}$	1.6	166
Benzothiazole	$\text{C}_7\text{H}_5\text{NS}$	14.9	1511
N-Cyclohexylformamide	$\text{C}_7\text{H}_{13}\text{NO}$	4.4	451
N-Cyclohexylacetamide,	$\text{C}_8\text{H}_{15}\text{NO}$	1.7	175
N-Cyclohexylcyclohexanamine	$\text{C}_{12}\text{H}_{23}\text{N}$	40.5	4113
N-Cyclohexylidenecyclohexanamine	$\text{C}_{12}\text{H}_{21}\text{N}$	0.4	44
N-methyl-[1,1'-Bicyclohexyl]-2-amine	$\text{C}_{13}\text{H}_{25}\text{N}$	4.4	443
N-Phenylcyclohexylamine	$\text{C}_{12}\text{H}_{17}\text{N}$	0.4	45
N,N'-Diphenylguanidine	$\text{C}_{13}\text{H}_{13}\text{N}_3$	1.9	197
Hexa(methoxymethyl)melamine	$\text{C}_{15}\text{H}_{30}\text{N}_6\text{O}_6$	17.1	1735

*based on the concentration of benzothiazole in leachate ($680 \pm 20 \text{ ug/L}$) and % of peak areas.

Table S3.

Conductivity and pH of crumb rubber water leachate, control water (LC/MS grade water), and tap water. The conductivity and pH of CR leachate are within the range in between those of control water and tap water.

	Control water	25%CR leachate	50% CR leachate	100% CR leachate	Tap water
pH (at 22°C)	6.95	7.20	7.28	7.34	7.86
Conductivity (μS/cm)	1.58	77.01	117.4	221.4	226.5

Table S4.

Primer sequences of selected genes.

Gene	GeneBank Acc. No.	F	R	Size	Average gene efficiency
HSP60	NM_0010 12916.1	AGCCAAAGGGCAGA AATG	TACAGCAACAACCT GAAGACC	208	0.80
HSP70	NM_0010 06685.1	CGGGCAAGTTTGAC CTAA	TTGGCTCCCACCCTA TCTCT	250	0.87
TR α	NM_2053 13.2	CAGCCAATGTTTGGT GAAGAG	GATGCAGCGGTAGT GGTAG	115	0.77
TR β	X17504.1	TCACACCAGCGATTA CAAGAG	ATCTCCATACAGCA GCCTTTC	109	0.82
TTR	NM_2053 35.3	GTTCTTACTGGAAGG GACTTGG	GGAGAGCAGCGATG GTATAATG	105	0.83
RC3	NM_0013 02155.1	CATGACCCGCAAGA AGATCAA	GGAGTCCAAGGAGG ACCTAAT	119	0.86
CYP1B1	JN656934	CATCTTCCTCATCAG GTATCCAAAAGT	GTACAGGAAAGCCA CGATGTAG	130	0.89
MT1	X06749.1	CTGCAACAACCTGTGC CAAG	CGAAGCATGGCAGC TATTTAC	107	0.83
CYP1A4	NM20514 7.1	ACTGCCAGGAGAAA AGGACAG	TCAAAGCCTGCCCC AAACAG	97	0.87
CYP1A5	NM20514 6.1	TTCACCATCCCGCAC AGCA	GTTTCTCATCGTGAT TCACTTGCC	109	0.85
AHR1	NM20411 8.1	GCTGTGATGCAAAA GGAAAGATTGTC	ATCCACTCTCACCC GTCTTC	148	0.92
EF1A	NM20415 7.2	GATGTCTACAAAATT GGTGGCATTGG	GCTTCATGGTGCATC TCAACAG	140	0.85

Table S5.

Chemical names with ion transitions and the MRM settings used for GC/MS analysis.

Name	CAS#	NIST ID#	Precursor ion (m/z)	Product ion (m/z)	Collision energy (eV)
Di-n-butylamine	111-92-2	454936	86.1	44.2	10
N,N-Dimethylcyclohexanamine	98-94-2	229064	127.1	84.2	5
Cyclohexylamine	108-91-8	290818	99.1	56.3	5
N,N-Dicyclohexylamine	101-83-7	290817	138.2	56.2	10
Benzothiazole	95-16-9	249193	135.2	108.1	25
N-Cyclohexylacetamide	1124-53-4	288932	141.1	60.2	5
N-Cyclohexylformamide	766-93-8	237814	84.2	56.2	10
N,N'-Diphenylguanidine	102-06-7	229823	93.0	66.2	15

References

1. P. Cignoni, M. Callieri, M. Corsini, M. Dellepiane, F. Ganovelli, G. Ranzuglia (2008) Meshlab: an open-source mesh processing tool. In Eurographics Italian chapter conference (Vol. 2008, pp. 129-136).
2. M. Corsini, P. Cignoni, R. Scopigno (2012) Efficient and flexible sampling with blue noise properties of triangular meshes. *IEEE Trans. Vis. Comput. Graph.* 18(6), 914-924.
3. M. Kazhdan, H. Hoppe (2013) Screened poisson surface reconstruction. *ACM Trans. Graph.* 32(3), 29
4. D.C. Adams, M. L. Collyer, A. Kaliontzopoulou (2018) Geomorph: Software for geometric morphometric analyses. R package version 3.0.6. <https://cran.r-project.org/package=geomorph>.
5. F. L. Bookstein (1989) Principal warps: Thin-plate splines and the decomposition of deformations. *IEEE Trans. Pattern Anal. Mach. Intell.* 11(6), 567-585.
6. A. Fedorov, R. Beichel, J. Kalpathy-Cramer, J. Finet, J. C. Fillion-Robin, S. Pujol, C. Bauer, D. Jennings, F. Fennessy, M. Sonka, J. Buatti, S. Aylward, J.V. Miller, S. Pieper, R. Kikinis (2012) 3D Slicer as an image computing platform for the Quantitative Imaging Network. *Magn Reson Imaging*, 30(9), 1323-1341.
7. OECD (2004) Test No. 202: *Daphnia* sp. Acute Immobilization Test, OECD Publishing, Paris. <https://www.oecd-ilibrary.org/docserver/9789264069947-en.pdf?expires=1568389332&id=id&accname=ocid195496&checksum=14338C6C5589F8DE94AC24AB977F729A>.